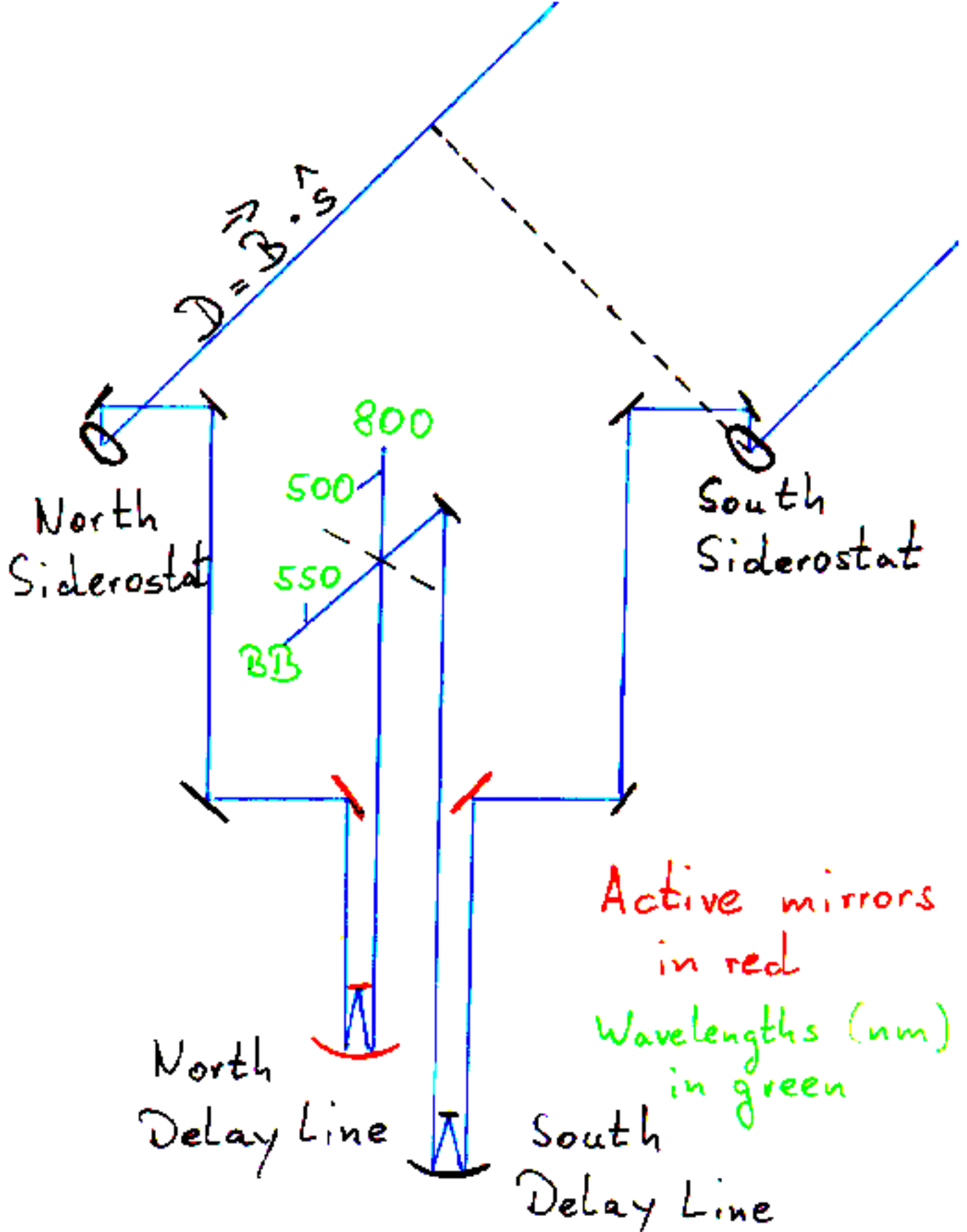


Phase Referencing

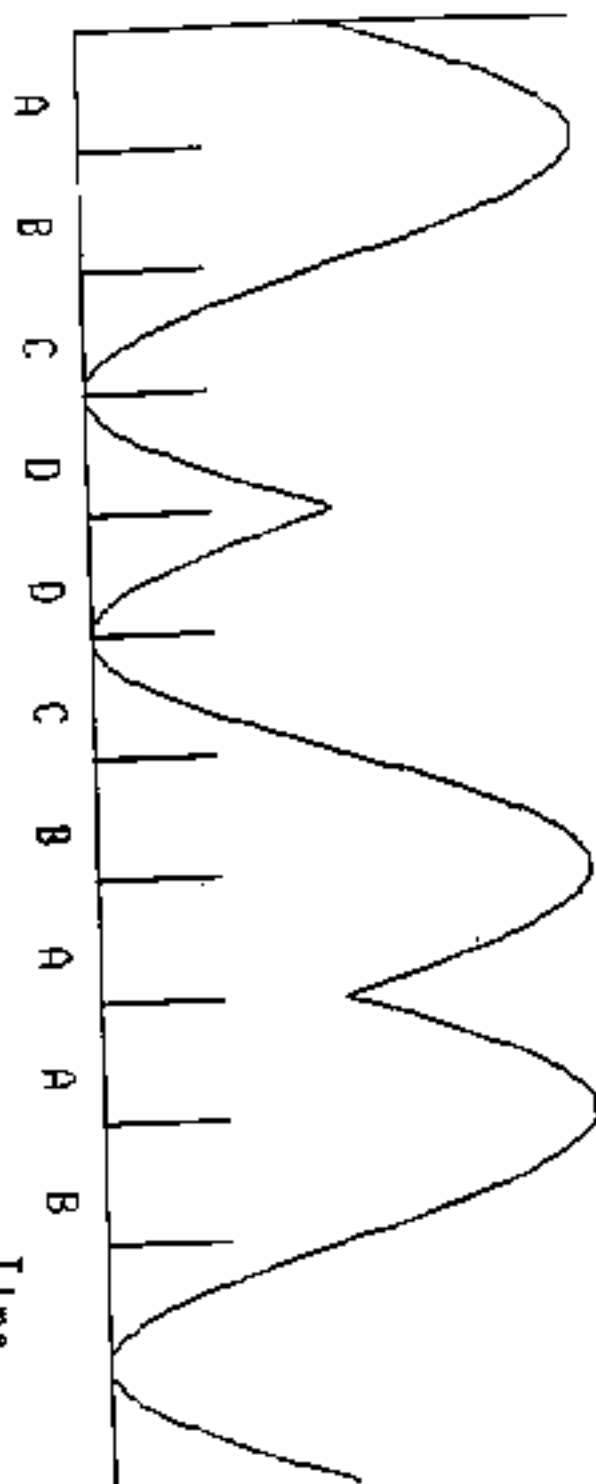
Andreas Quirrenbach

(University of California, San Diego)

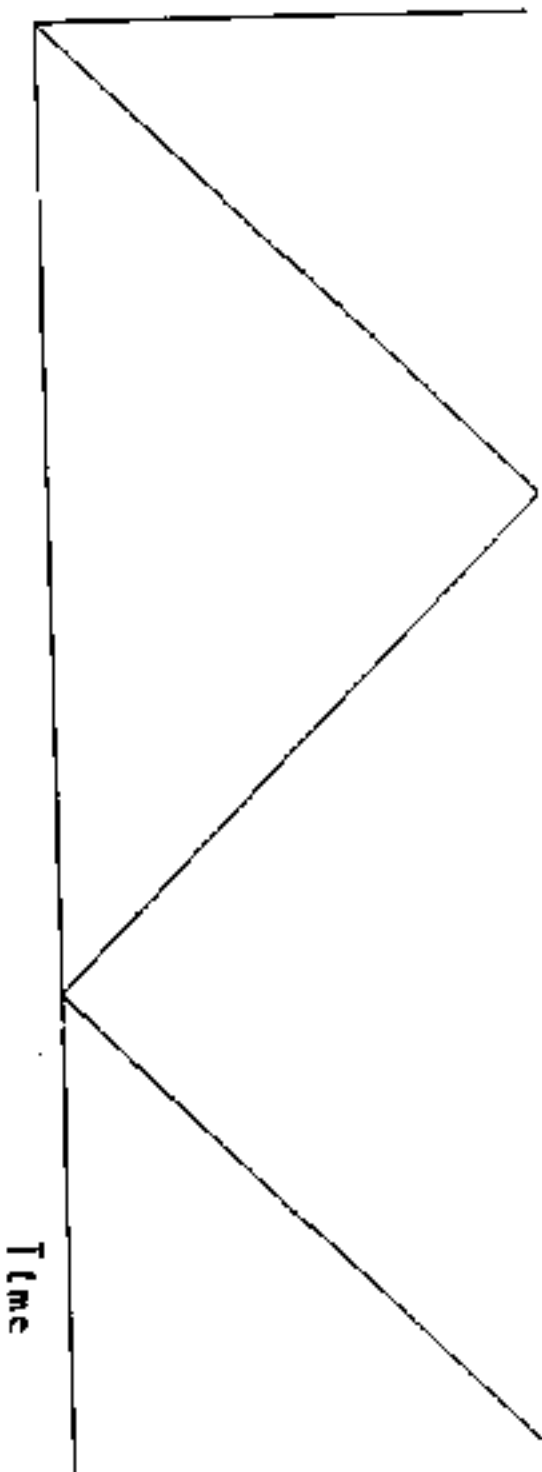




INTERFERENCE FRINGE



PATH MODULATION



Basic Fringe Quantities

Fringe sine and cosine: $X := A - C$ $Y := B - D$

Visibility: $V^2 = \frac{\pi^2}{2} \frac{\langle X^2 + Y^2 - N \rangle}{\langle N - N_{dark} \rangle^2}$

Phase: $\tan \phi = \frac{\langle Y \rangle}{\langle X \rangle} - \frac{\pi}{4}$

Signal-to-noise: $SNR = \frac{1}{4} \frac{\sqrt{M} NV^2}{\sqrt{1 + 0.5 NV^2}}$

Photon-Rich and Photon-Starved Observations

- Photon-rich regime: $NV^2 \gg 1$

$$\text{SNR} \propto \sqrt{MN} \propto \sqrt{t_{\text{obs}}}$$

- Photon-starved regime: $NV^2 \ll 1$

$$\text{SNR} \propto \sqrt{M} \times N = \sqrt{MN} \times \sqrt{N} \propto \sqrt{t_{\text{obs}}} \times \sqrt{t_{\text{coh}}}$$

- The bottom line: you need two photons to do interferometry!
- Sensitivity of interferometer is limited by the number of photons in coherence volume (e.g., $\frac{\pi}{4} r_0^2 \times c \tau_0$)

Table Ib. Source-referenced Mode Sensitivity
Phasing & Cophasing. *Long-Term Case*
Telescope Diameter 2-m

Seeing	H	K	L	M	N	Q
0.5"	11.2	12.3	10.4	8.1	5.3	2.4
	35	8	21	110	320	1 100
1.0"	8.9	10.1	8.5	6.7	4.9	2.0
	280	59	120	390	460	1 600

Units: upper lines are magnitudes ; lower are milliJy

Phasing: $V = 1$ or $V \neq 1$. Cophasing: $V = 1$.

1.0" seeing $\Leftrightarrow r_o(0.5\mu\text{m}) = 10$ cm.

Table Ib. Source-referenced Mode Sensitivity
Phasing & Cophasing. *Long-Term Case*
Telescope Diameter 8-m

Seeing	H	K	L	M	N	Q
0.5"	11.2	12.3	10.4	8.6	7.6	5.4
	35	8	21	69	38	70
1.0"	8.9	10.1	8.5	6.7	5.8	4.5
	280	59	120	390	210	150

Units: upper lines are magnitudes ; lower are milliJy

Phasing: $V = 1$ or $V \neq 1$. Cophasing: $V = 1$.

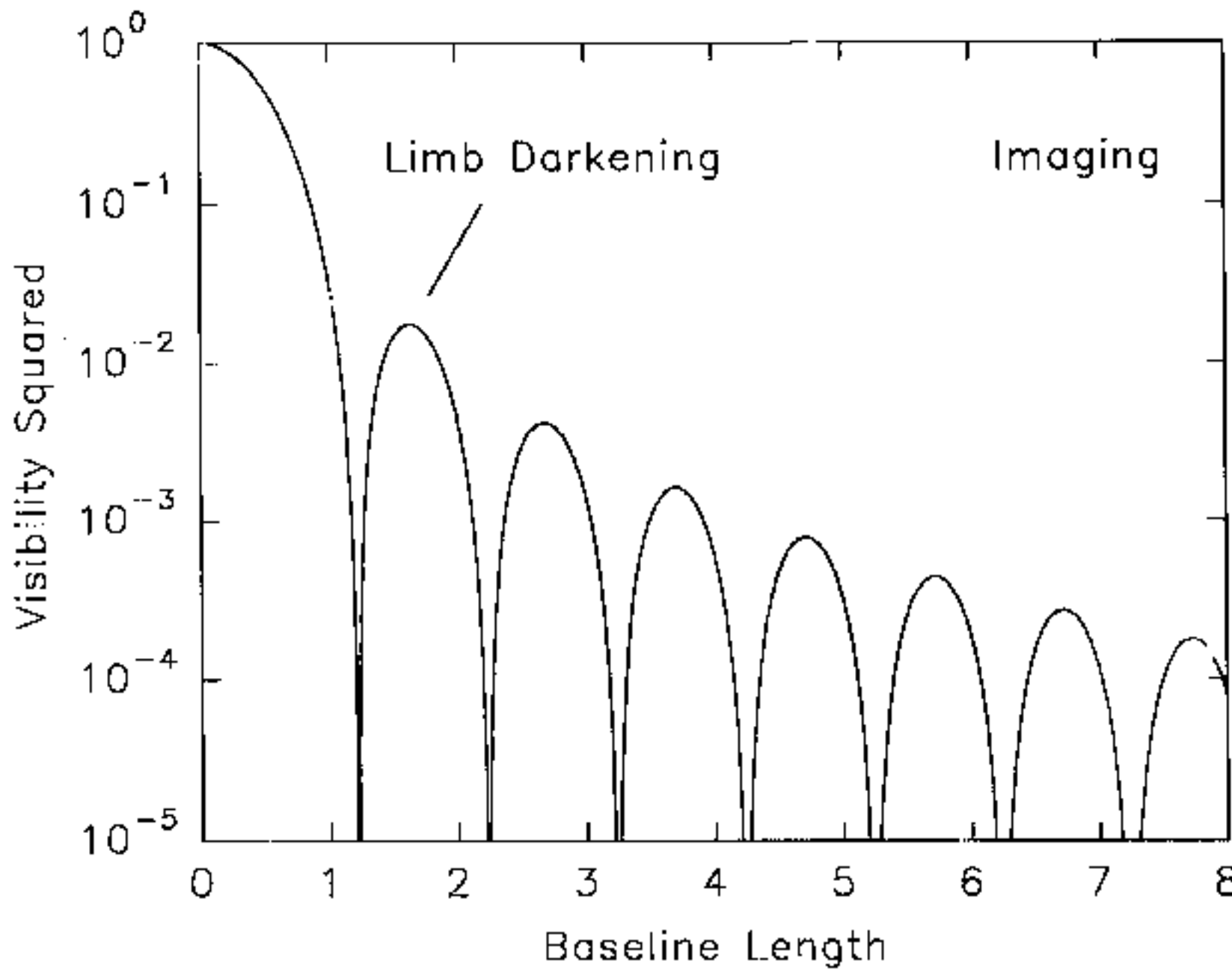
1.0" seeing $\Leftrightarrow r_o(0.5\mu\text{m}) = 10$ cm.

Table III. Off-source Referenced Mode Sensitivity
Integration Time $\Delta T = 10$ minutes. *Long Term case*

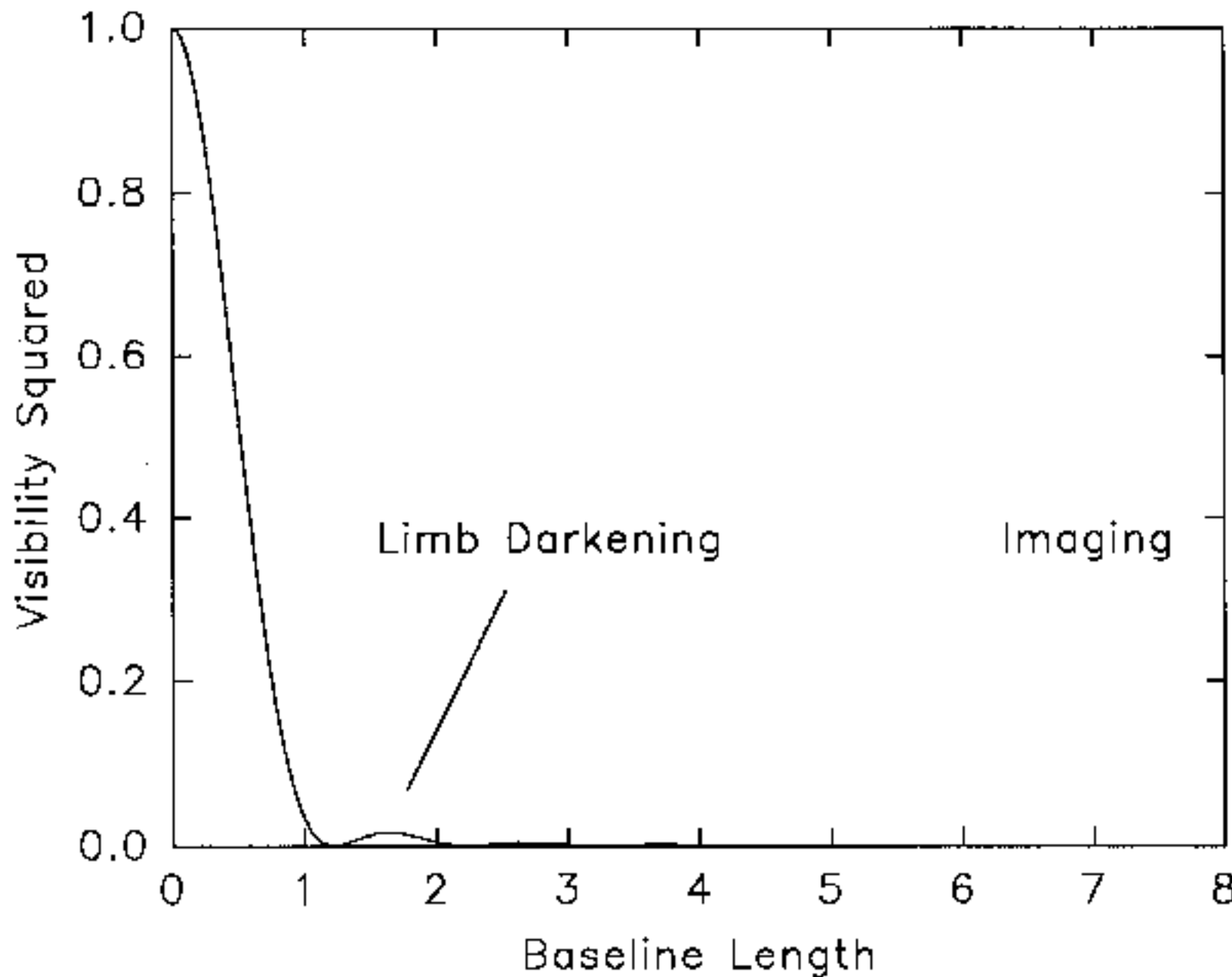
Telescope	H	K	L	M	N	Q
2-m + 2-m	21.1	20.4	15.3	12.2	8.9	5.6
	.004	.005	.24	2.5	11	59
8-m + 8-m	24.1	23.4	18.3	15.2	11.9	8.6
	.0002	.0003	.015	.15	.72	3.7

Units: upper lines are magnitudes ; lower are milliJy

Uniform Disk (Airy Function)



Uniform Disk (Airy Function)



Fringe Tracking

Fringe tracking requires $\text{SNR} \gtrsim 10$ *within one coherence time of the atmosphere* (a few milliseconds in the visible, scales with $\lambda^{6/5}$).

What can be done if NV^2 is too small?

- Wavelength bootstrapping or baseline bootstrapping gives larger V^2 on the same source.
- Off-source fringe tracking can be used if a bright reference is available.

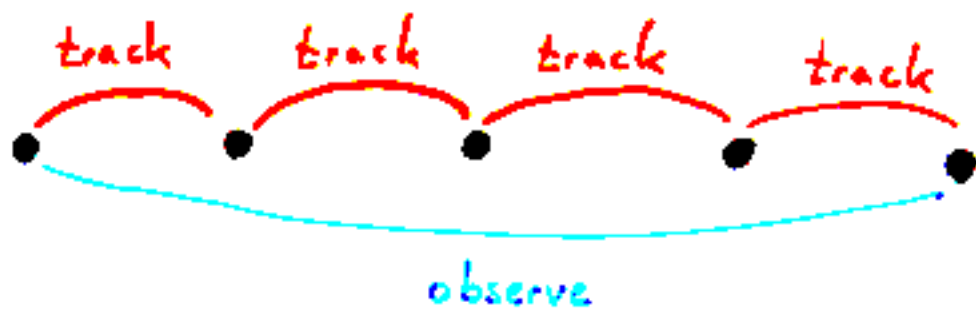
Off-Source Fringe Tracking

The reference source must be within the isoplanatic field of the science target (a few arcseconds in the visible, scales with $\lambda^{6/5}$).

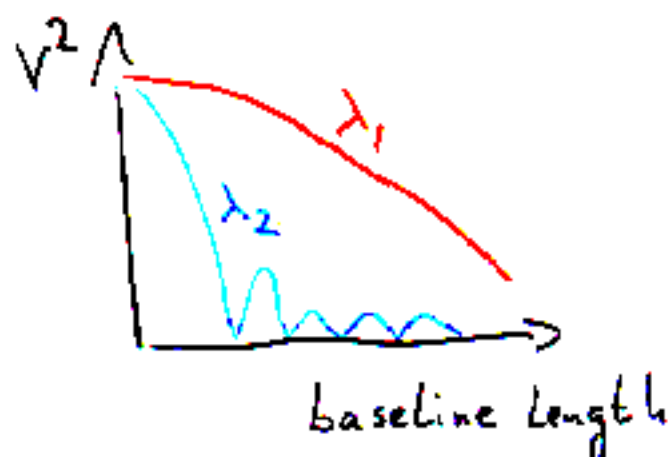
The reference source can also be used for wavefront sensing in an adaptive optics system.

In this case the sensitivity of the interferometer is essentially identical to the sensitivity of a single telescope with the same diameter.

baseline bootstrapping



wavelength bootstrapping



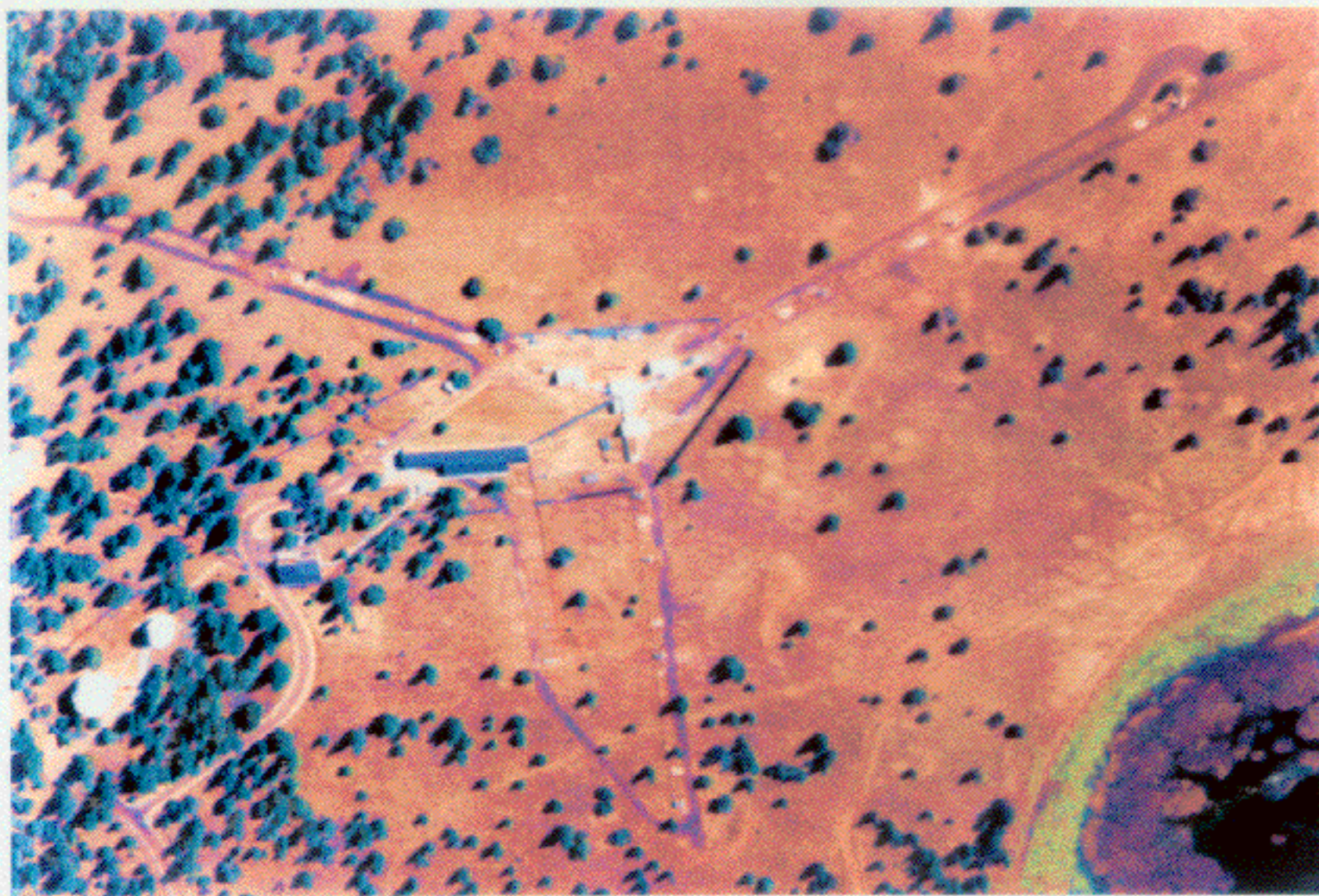
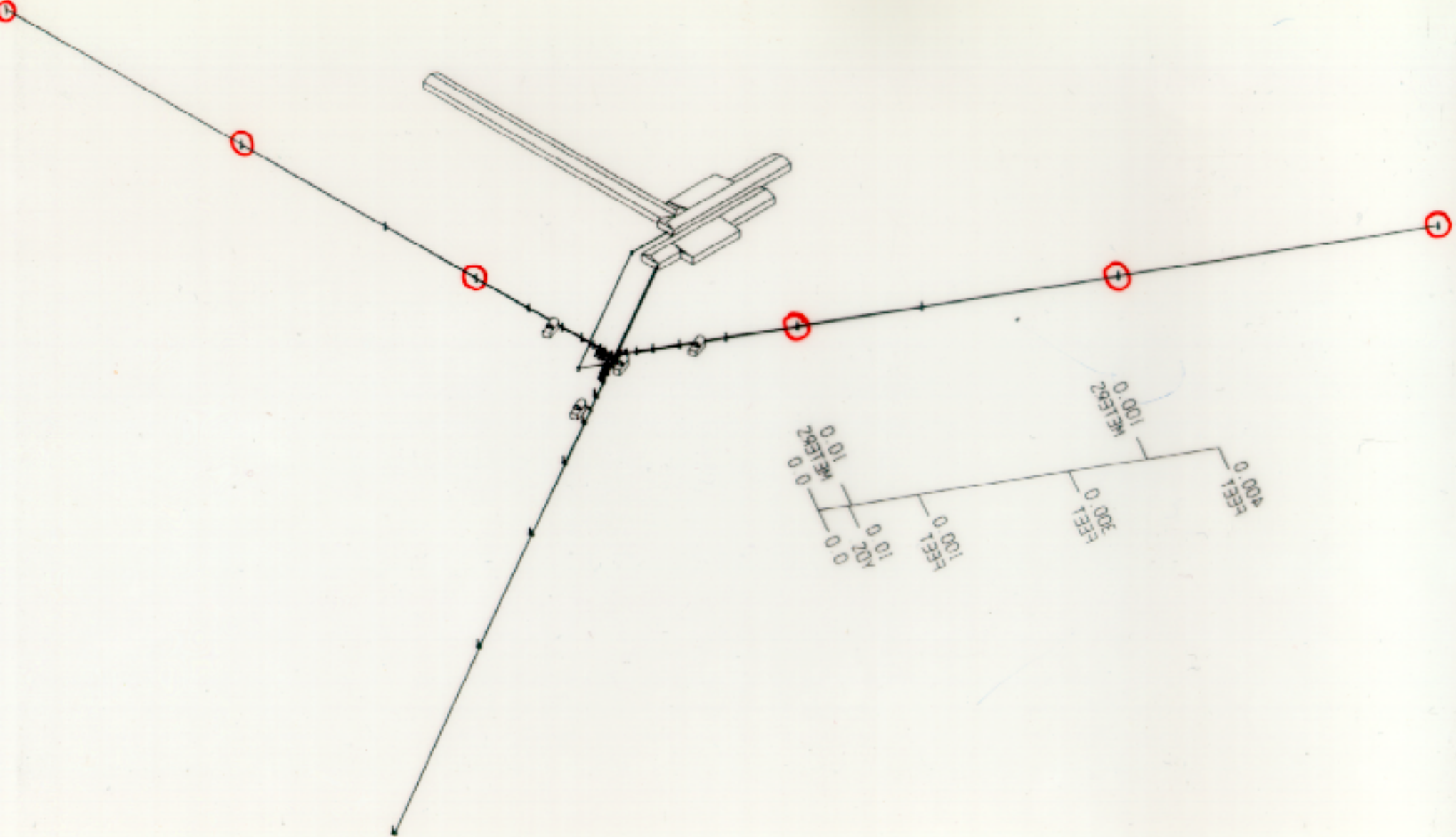


FIG. 1.—Aerial view of the NPOI as of 1996 October. North is toward the top of the photograph. Along the arms of the Y, small piers to support the feed beam vacuum pipes and larger piers to support the imaging siderostats can be seen. The farthest imaging siderostat piers are 250 m from the center of the array. The cluster of four white buildings at the center houses the four astrometric siderostats. The long building is the optics laboratory. Stretching north from the east end of the lab is the array of concrete piers on which the long delay lines will be placed. The control building is northwest of the lab. Also visible are two Lowell Observatory domes.

ARMSTRONG et al. (see 496, 551)

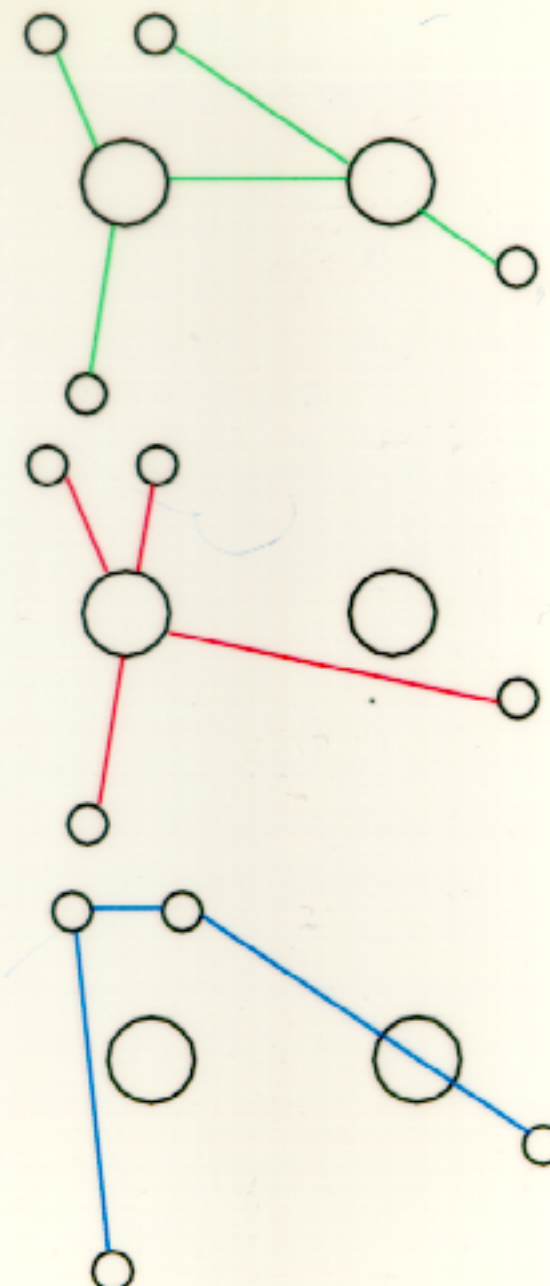




KECK
INTERFEROMETER

Imaging - technical

- Maximum 6 telescopes
- Cophase on max. 6-1 baselines at H/K, on bright point source
- Image on max. 15 baselines



Applications of Phase Referencing

- Off-axis phasing of interferometer on nearby guide star
- Observation in narrow wavelength channel with fringe tracking in wide channel
- Observation in wavelength channel with low visibility (a.k.a. wavelength bootstrapping)
- Observation on long baseline with fringe tracking on short baselines (a.k.a. baseline bootstrapping)
- Measurement of phase shift as a function of wavelength

Phase-referenced visibility averaging in optical long-baseline interferometry

A. Quirrenbach^{1,2,3}, D. Mousikewich^{1,4}, D.F. Buscher^{1,2}, C.A. Hummel^{1,2}, and J.T. Armstrong^{1,2}

¹ NRL/USNO Optical Interferometer Project, U.S. Naval Observatory, A.D.S., 3450 Massachusetts Avenue, NW, Washington, DC 20391-5420, USA

² Universities Space Research Association (USRA), 300 C Street, SW, Suite 801, Washington, DC 20024, USA

³ present address: Max-Planck-Institut für Extraterrestrische Physik, Giessenbachstr., D-85748 Garching, Germany

⁴ Remote Sensing Division, Naval Research Laboratory, Code 7243, Washington, DC 20375, USA

Received 8 December 1993 / Accepted 19 February 1994

Abstract. In the photon-starved regime, the signal-to-noise ratio of interferometric data depends on the coherent integration time. To extend the integration time beyond the limit imposed by atmospheric fluctuations, the phases taken in a narrow "signal" channel can be corrected by referencing them to those taken in a wider "tracking" channel. A number of instrumental and atmospheric effects decorrelate the phases in the two channels and thus constrain the range of conditions under which the phase-referencing technique can be used. In the case of the MkIII stellar interferometer, differential refraction at intermediate to large zenith angles is the most important limitation. Tests with MkIII data in the photon-rich regime demonstrate that the phase-referencing technique works well at moderate zenith angles. In the photon-starved regime, the expected improvement of the signal-to-noise ratio is readily observed. We use phase-referenced data taken on the bright star α Boo close to the first null of the visibility function to show that the MkIII data are free from additive bias at the $V^2 \leq 10^{-4}$ level. The absence of any bias larger than this value is an important requirement for future imaging Interferometers.

Key words: atmospheric effects – instrumentation: interferometers – methods: observational – methods: data analysis – techniques: interferometric

phase information from a reference object is used to determine the atmospheric phase, and to correct the phase of the target source accordingly.

While in radio astronomy the atmospheric coherence time is typically several minutes, and the coherence angle several degrees, the corresponding values in the optical regime are only of order ten milliseconds and a few arcseconds. These limitations preclude the use of source-switching strategies and require the simultaneous observation of target and reference object. While this might appear to be a very restrictive requirement, there are several important applications of phase-referencing to optical long-baseline interferometry. First, the phase difference can be used as a primary observable in "astrometric" applications, e.g. to determine the positional offset of a circumbinary envelope from the central star, or to search for the reflex motion of stars orbited by planets. (In the latter case, a suitable reference object is needed within the isoplanetary patch.) Second, the reference phase can be used to increase the effective atmospheric coherence time, allowing longer coherent integrations on the target source.

In this paper, we will discuss the coherent integration of visibility amplitudes in a "narrow" spectral channel, using the phase in a broader channel as a reference. This technique will be applied to data taken with the MkIII interferometer¹. In Sect. 2 we will summarize the most important features of the MkIII instrument and describe the phase-referencing algorithm. In Sect. 3 we will review the sources of systematic errors and fundamental limitations to the technique. In Sect. 4 we will describe a test of phase-referencing using data with high signal-to-noise and compare the results with theoretical predictions. In Sect. 5 we will show the application of the algorithm to data with low signal-to-noise. Finally, we will summarize the results and discuss some future applications in Sect. 6.

¹ The MkIII Optical Interferometer located on Mt. Wilson near Los Angeles, CA, is operated by the Remote Sensing Division of the Naval Research Laboratory (NRL).

1. Introduction

The use of phases in astrometric interferometry is severely limited by the pathlength fluctuations of the earth's atmosphere. Two different approaches are widely used to deal with the problem of phase corruption: closure phase methods (or phase self-calibration), and phase-referencing. In the latter technique, the

Send offprint requests to: A. Quirrenbach (Garching address)

Visibility Reduction

- Phase variations during the coherent integration time reduce the visibility
- If σ_ϕ^2 is the phase variance, $V^2 \rightarrow \eta V^2 = e^{-\sigma_\phi^2} V^2$
- Solution 1: keep phase variations small (requires many photons and fast servo for fringe tracking)
- Solution 2: break up total observing time in sections small enough to show no phase variations (incurs a signal-to-noise penalty)
- Solution 3: determine and correct phase fluctuations

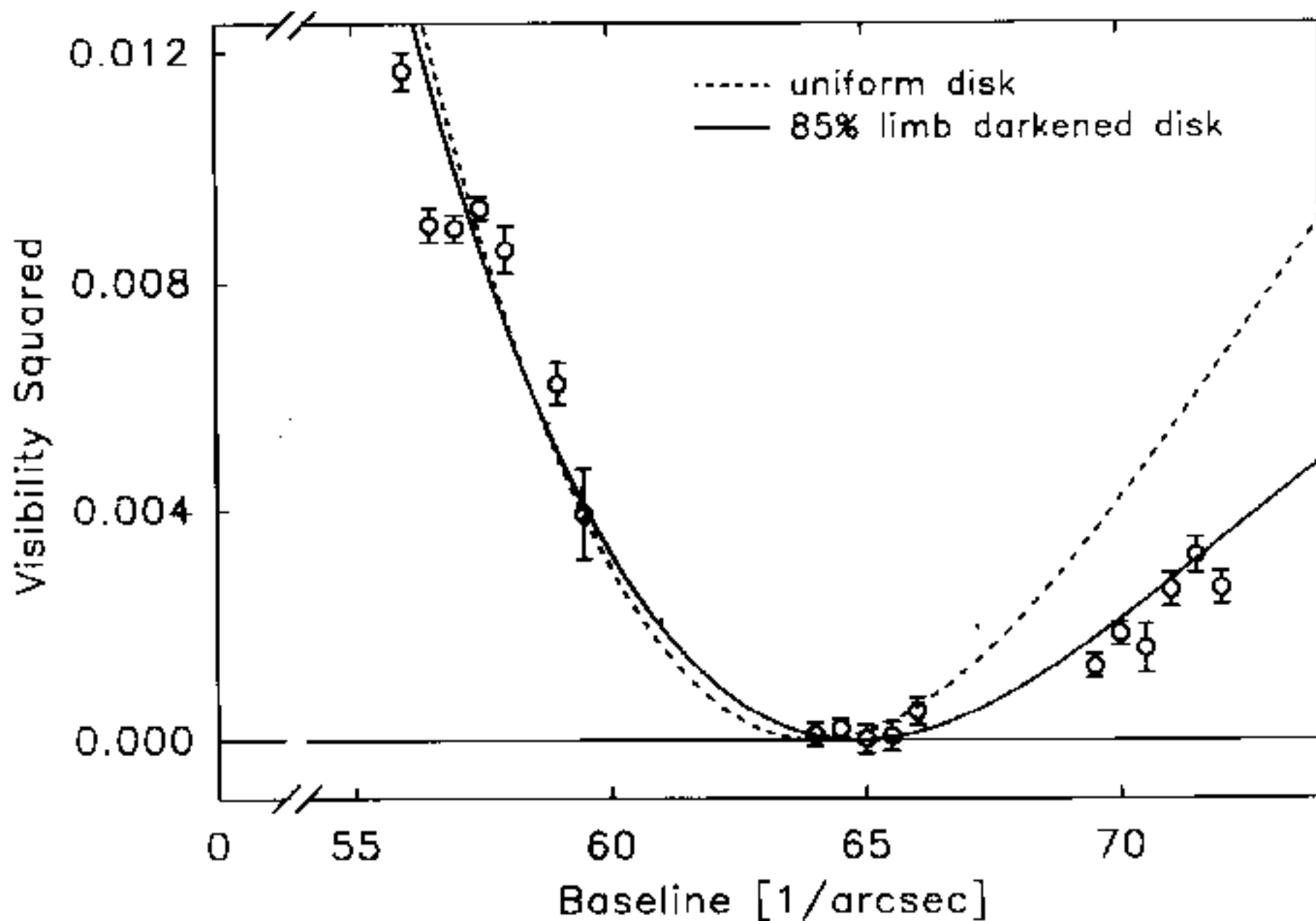
Mark III: Incoherent Averaging

- Feed fringe tracker with wide-band light (centered at 700 nm)
- Get bin counts A, B, C, D in narrow signal channel for many 4 ms intervals
- Estimate V^2 from bin counts for each interval
- Average estimates of V^2 for each scan (75 s to 300 s)

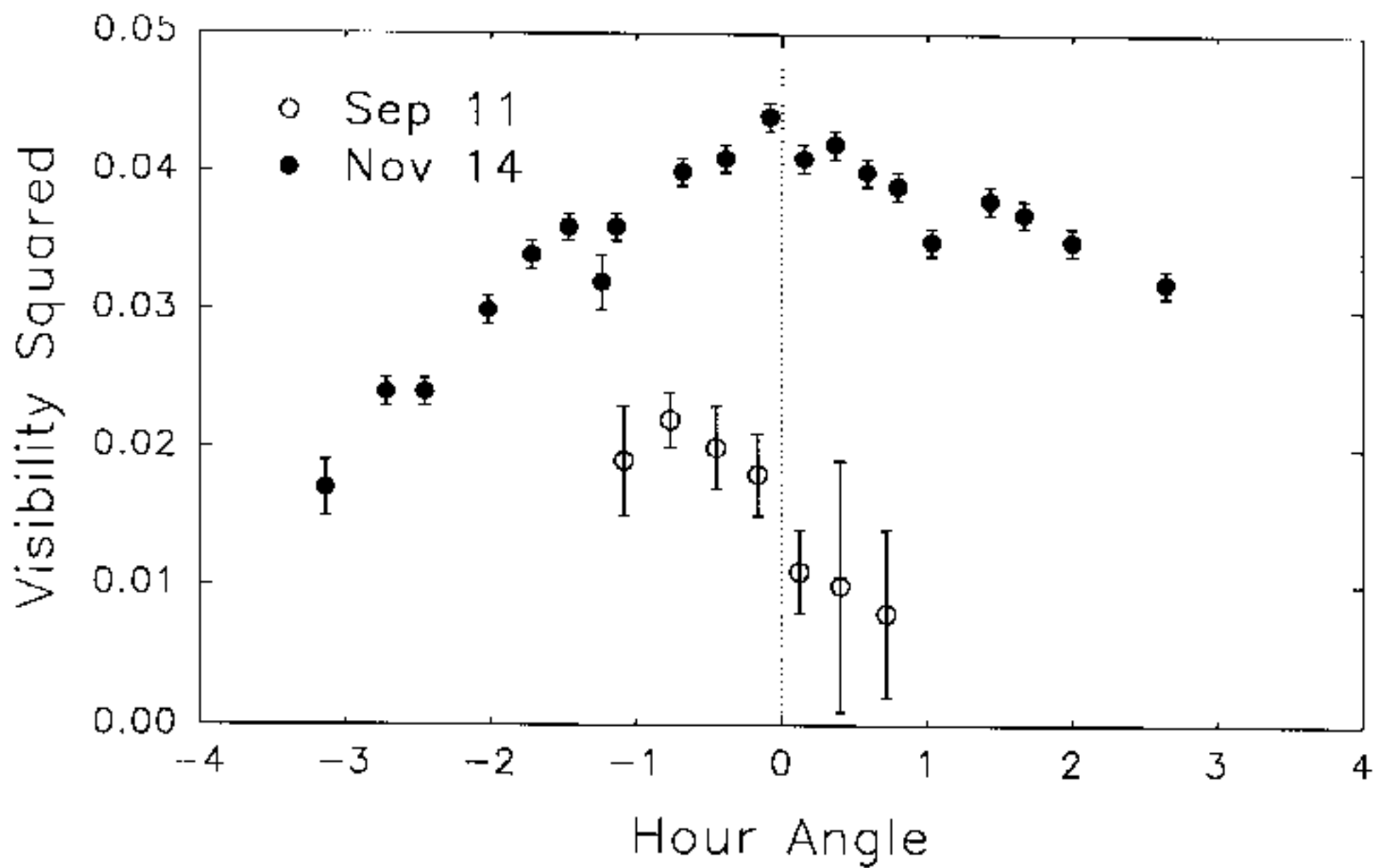
Mark III: Phase-Referenced Averaging

- Feed fringe tracker with wide-band signal (centered at 700 nm)
- Get bin counts A, B, C, D in signal and tracking channels for many 4 ms intervals
- Estimate phases ϕ_s and ϕ_t in signal and tracking channels for each 4 ms interval
- Define $X_r + iY_r = V_r e^{i\phi_r} \equiv V_s e^{i(\phi_s - \frac{\lambda_t}{\lambda_s} \phi_t)}$
- Average X_r and Y_r for up to 1024 ms; calculate V^2 for each of these intervals
- Average V^2 for each scan (75 s to 300 s)

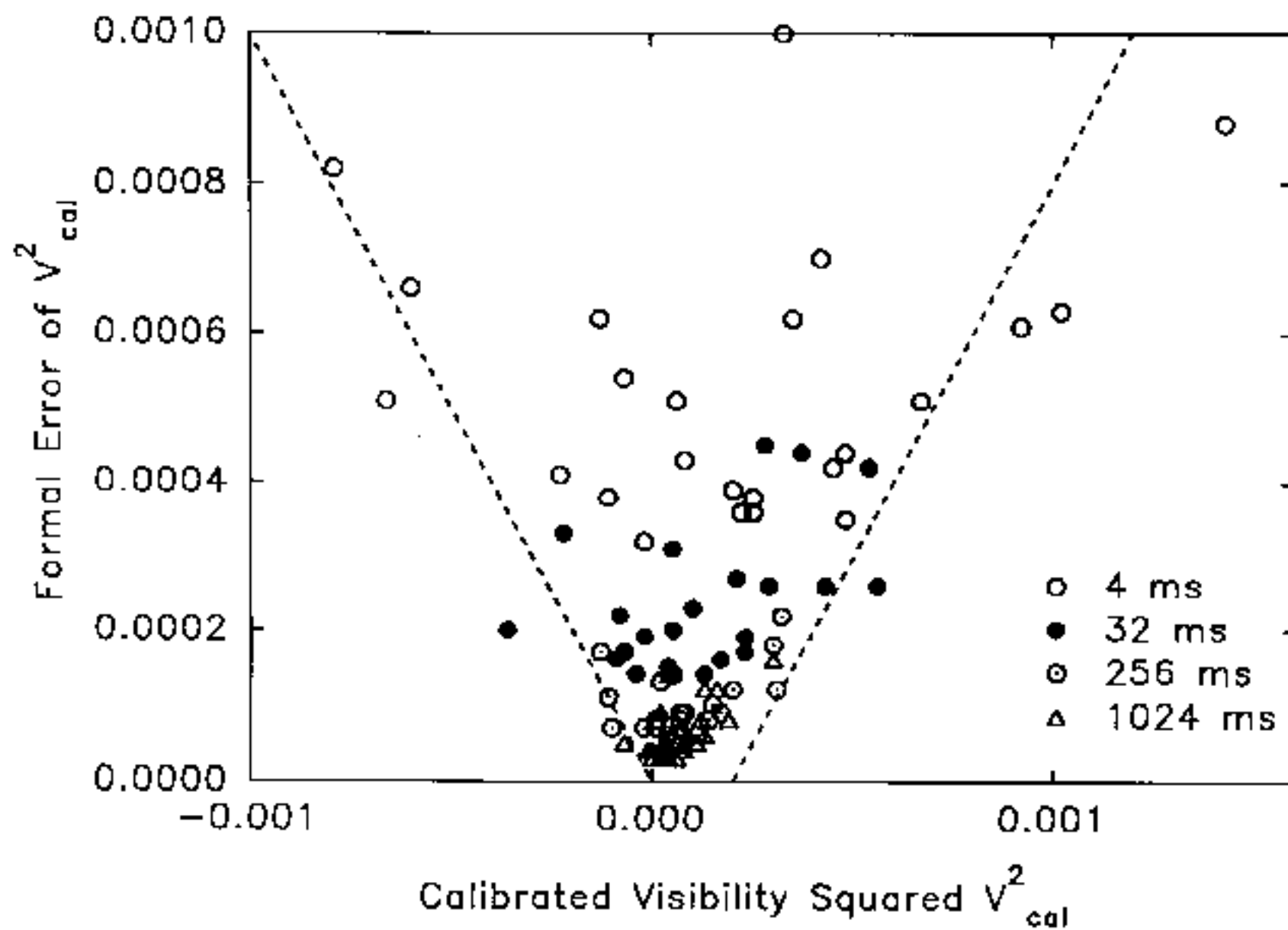
Alp Boo 550 nm



Mira 6.6 m Baseline 1990



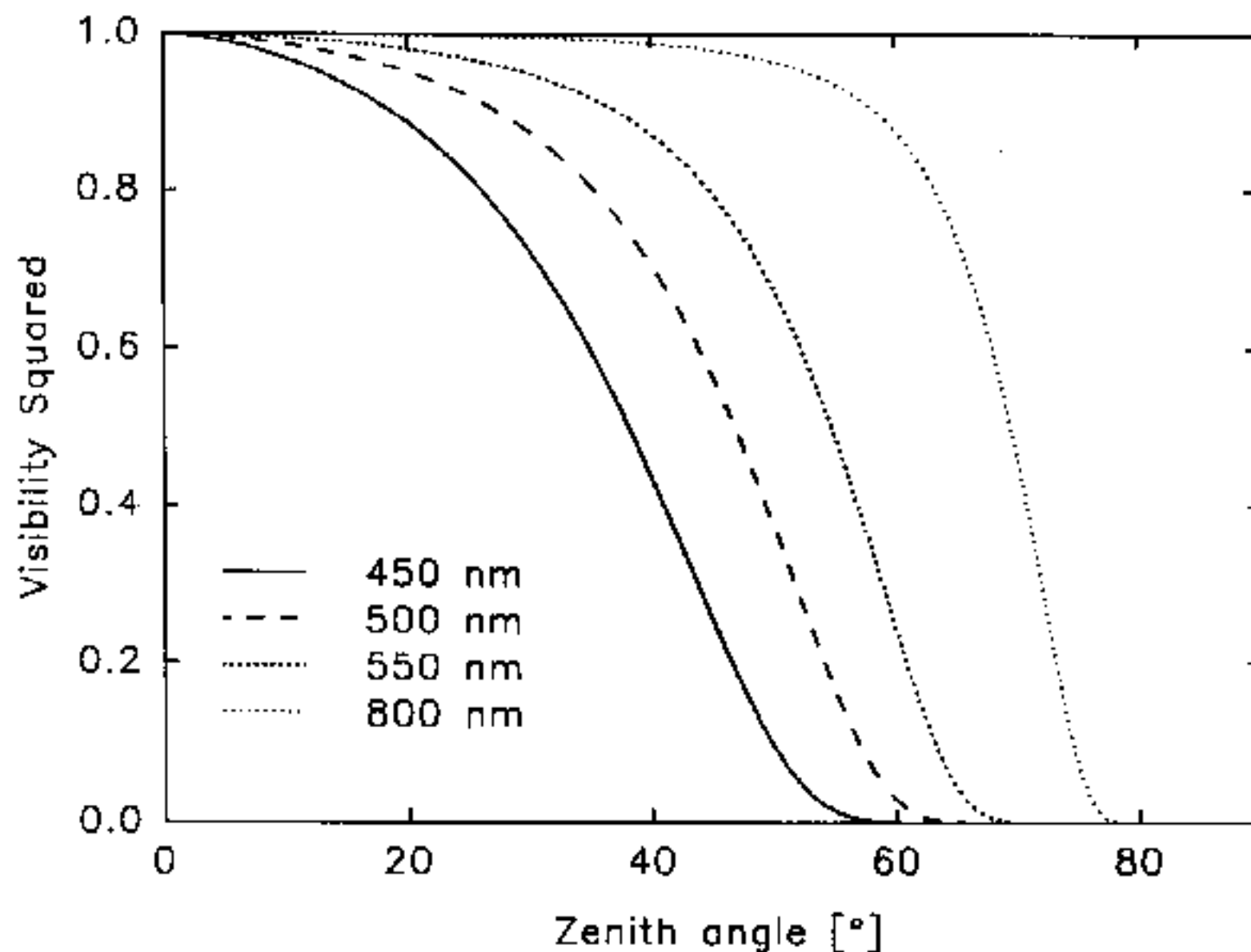
Arcturus 550 nm.



Decorrelation Effects

- Photon noise in tracking channel
- Color and visibility dependence of effective tracking wavelength
- Stroke mismatch (A, B, C, D don't correspond exactly to $\lambda/4$)
- Fringe jumps ($\phi_t \rightarrow \phi_t \pm 360^\circ$)
- Dispersion ($\phi_{\text{atm}, s} \neq \frac{\lambda_t}{\lambda_s} \phi_{\text{atm}, t}$), can approximately be taken into account in definition of referenced phase)
- Anisoplanatism (if tracking on off-axis source)
- Differential refraction (light at λ_t and λ_s takes different paths)
- Diffraction

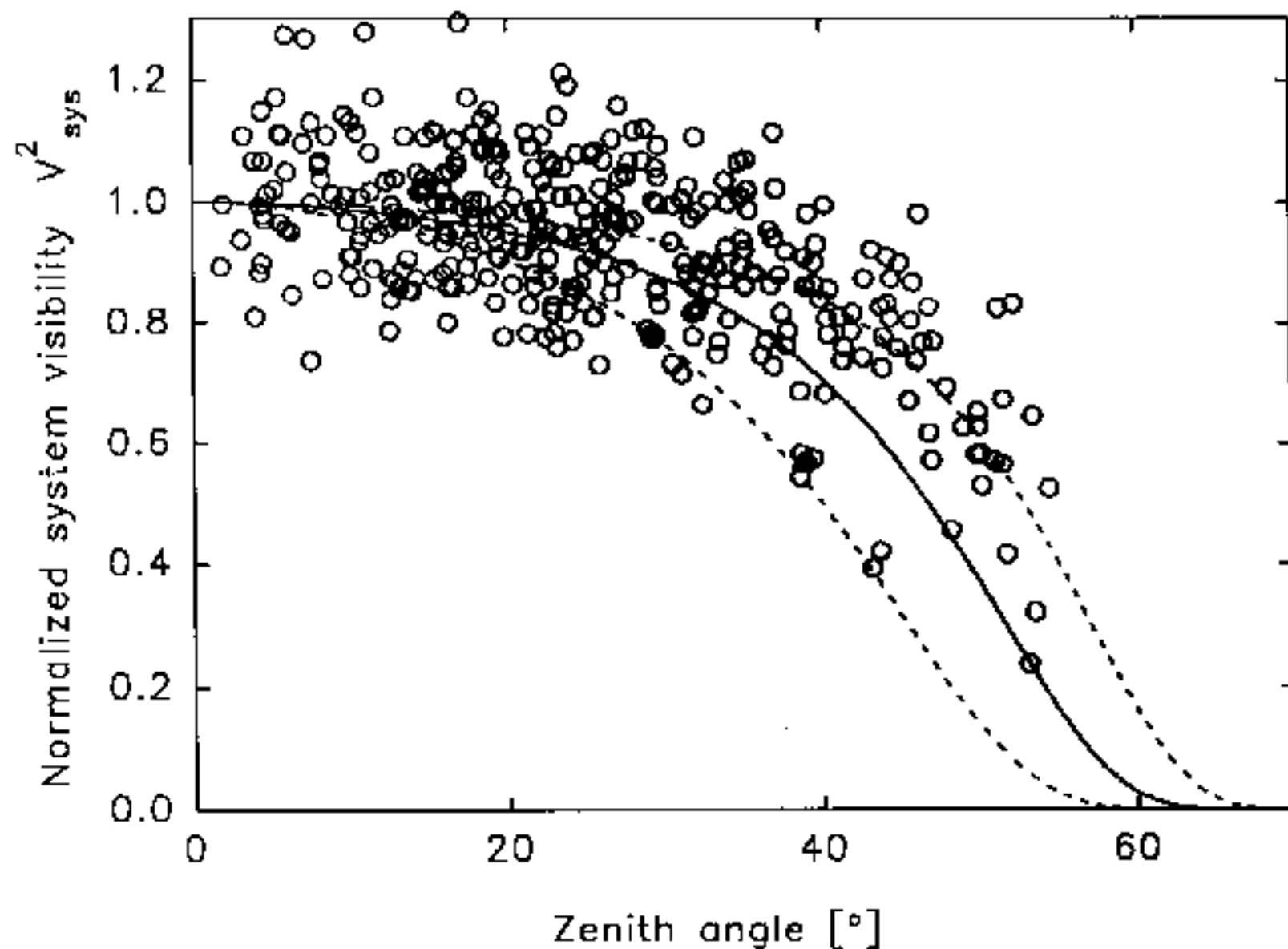
Hufnagel model atmosphere 700 nm reference



1024 ms Integration

500 nm Data

Hufnagel model



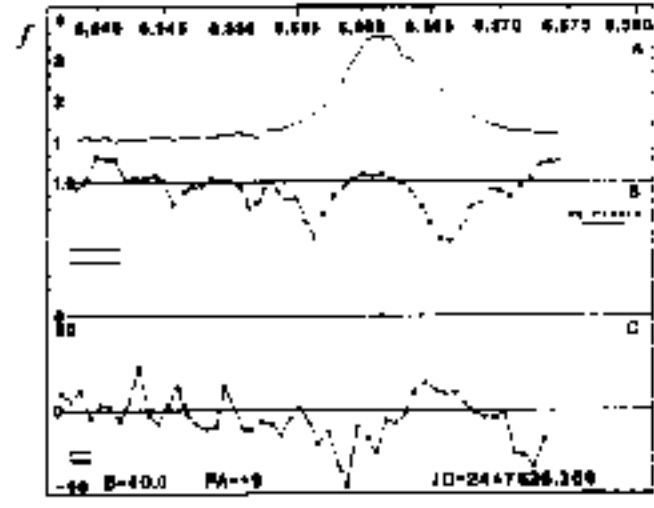
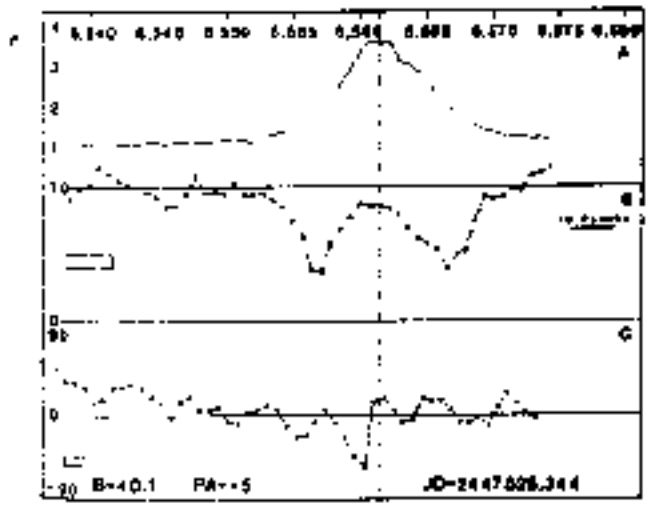
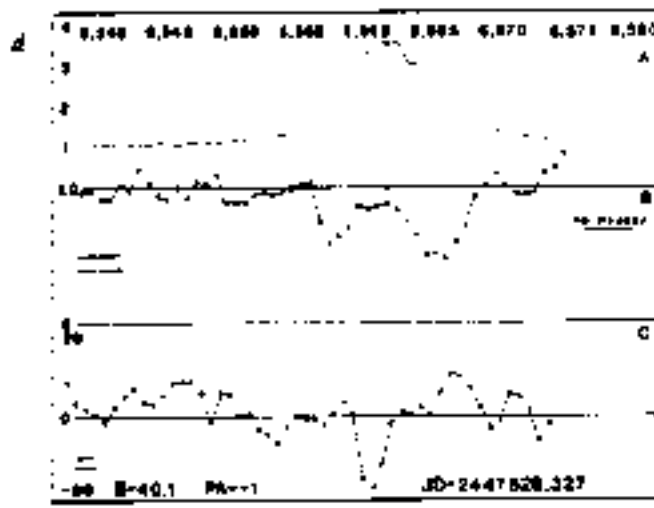
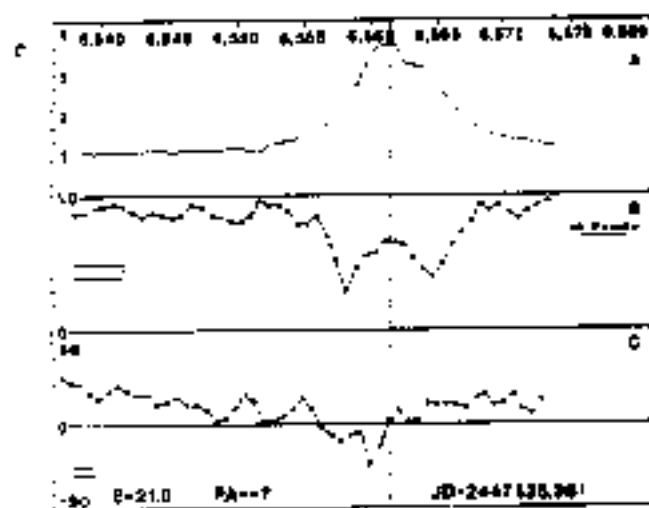
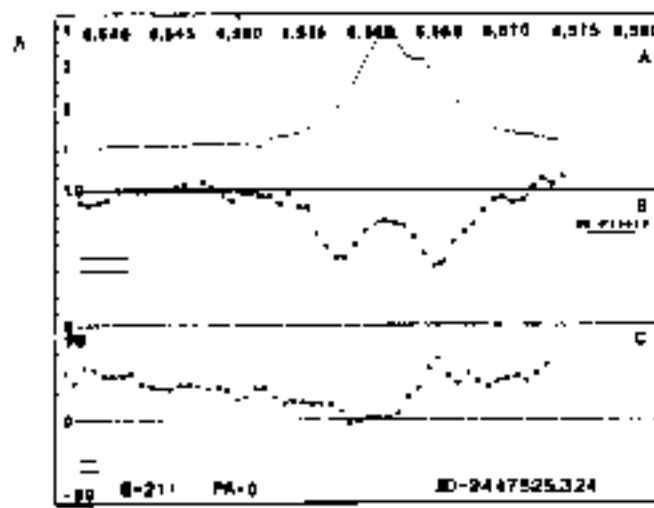
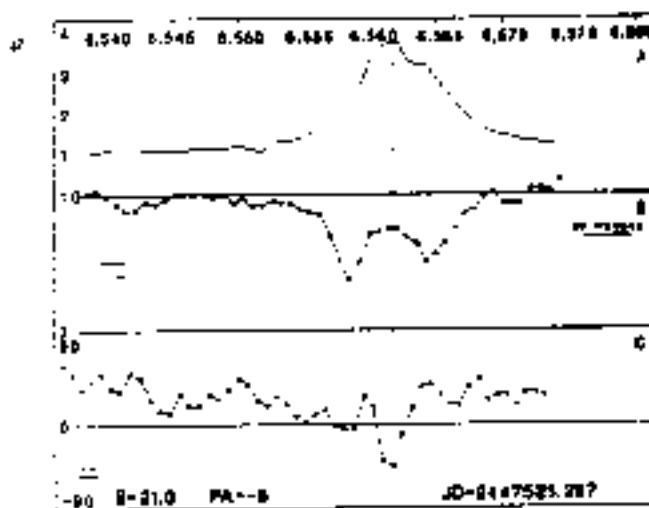


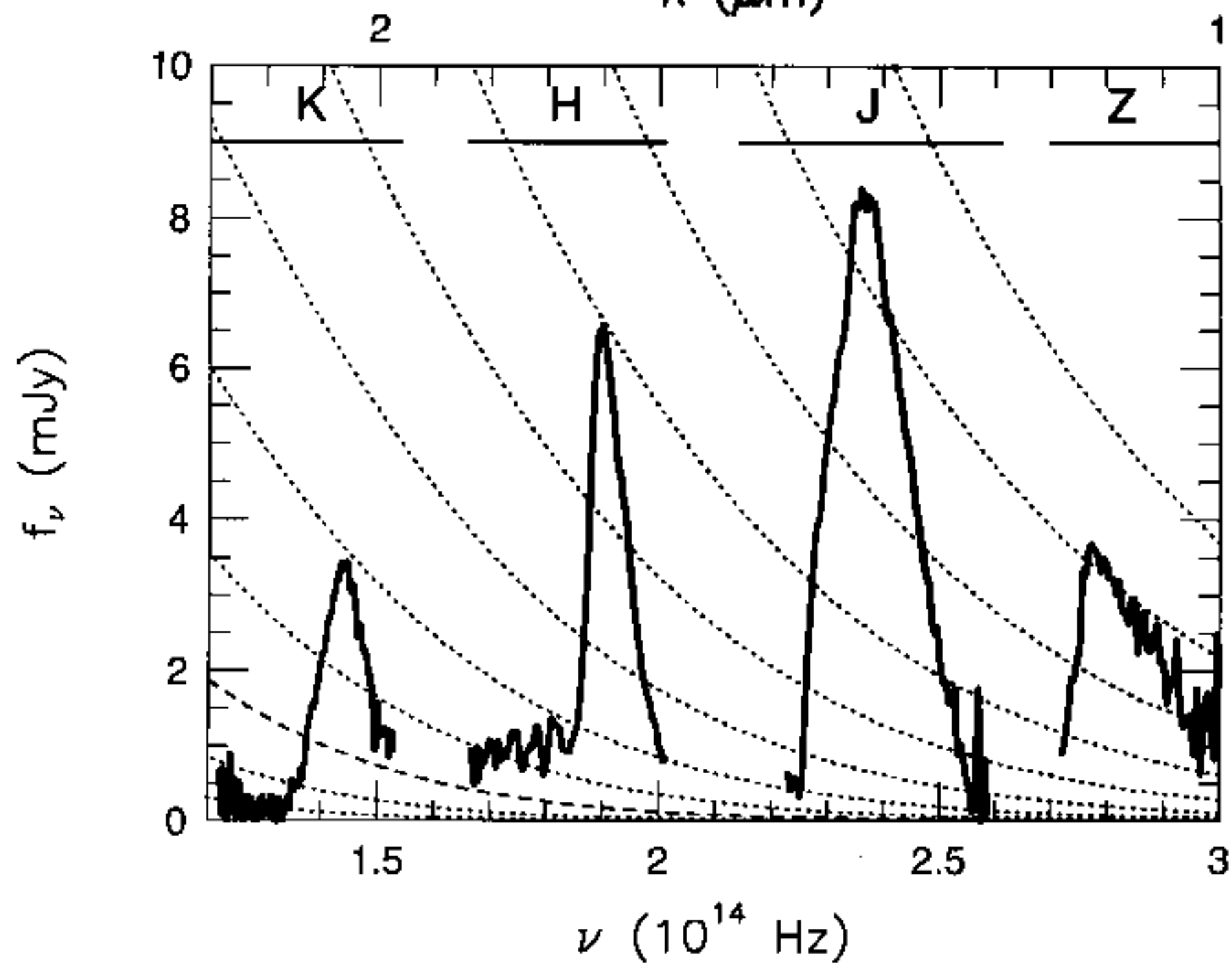
FIG. 1 Spectrum (A), with relative visibility modulus (B) and phase (C) as a function of wavelength, across the hydrogen alpha emission of γ -Cas. B (in meters) is the baseline projected on this sky. PA (in degrees, from north to west) the position angle of the baseline and JD the julian date of the observation. The visibility drop in both wings of the line is evidence for a hydrogen structure rotating with high velocities. Among the noisy phase curves, a significant disturbance also occurs at the line position. Because

the line profile varied markedly from night to night, differences between corresponding curves may be linked to the changing morphology. The uncertainty boxes shown indicate, vertically, the r.m.s. noise level and, horizontally, the width of the sliding window used to reduce the spectral resolution. The signal-to-noise ratio is approximately twice as good at the centre of the line owing to the higher photon count.

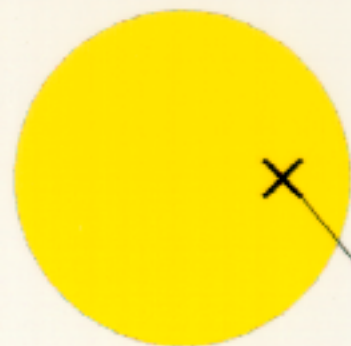
GL 229 B

λ (μm)

Matthews et al. (1996)



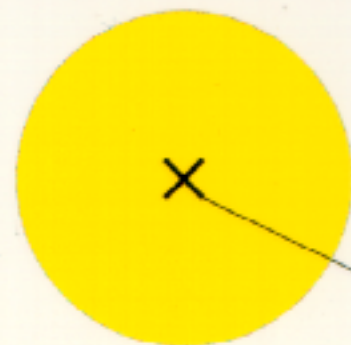
outside molecular band



photocenter



inside molecular band



photocenter

KECK INTERFEROMETER CDR

Keck DSM

Adaptive
Optics
Bench
(AOB)

Secondary Field
Steering Mirror

Field Separator with 10 arcsec dia. hole

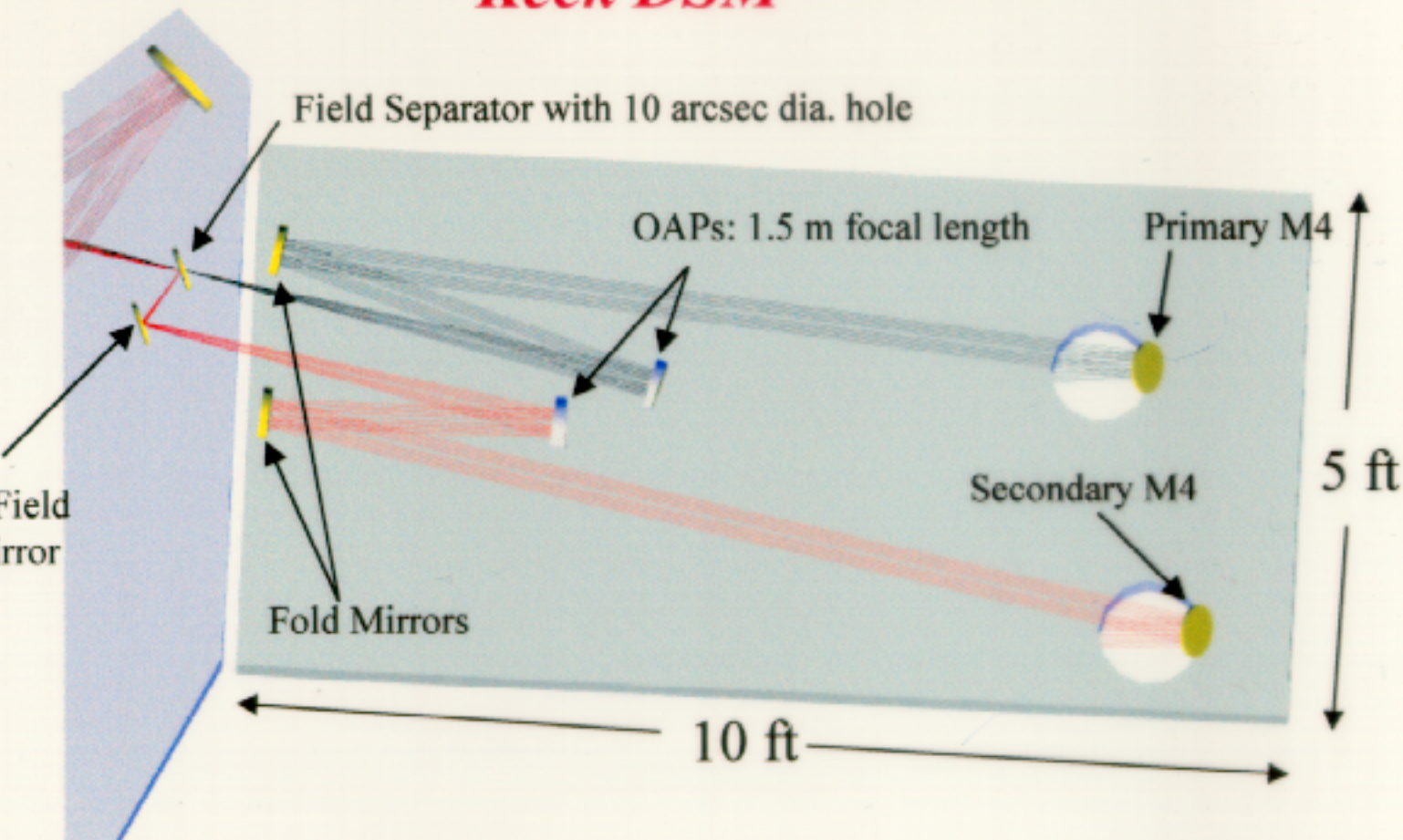
OAPs: 1.5 m focal length

Primary M4

Secondary M4

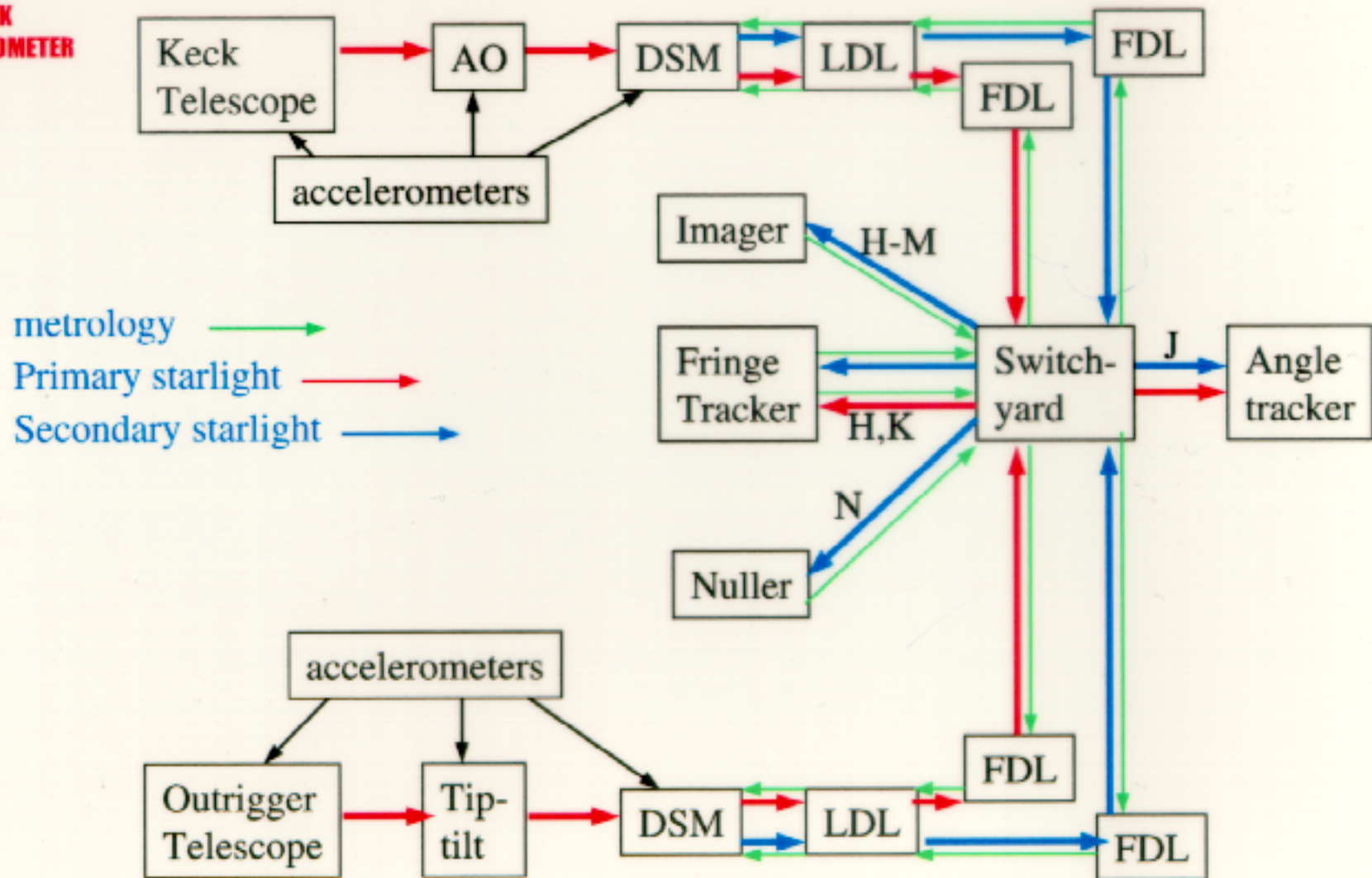
5 ft

10 ft

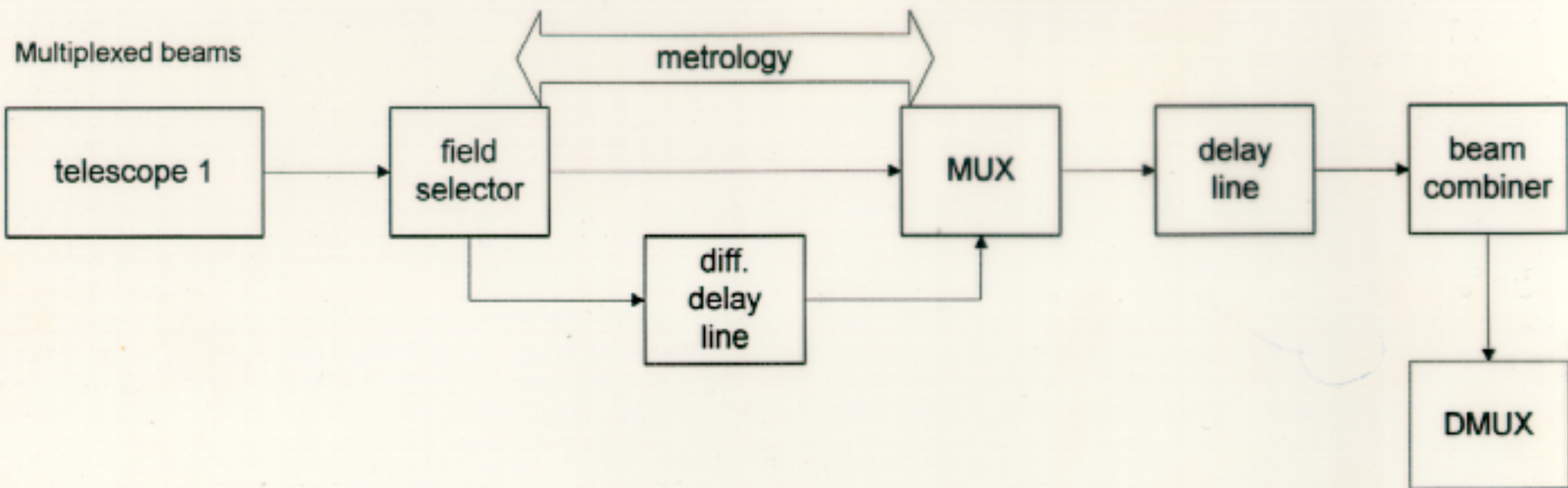




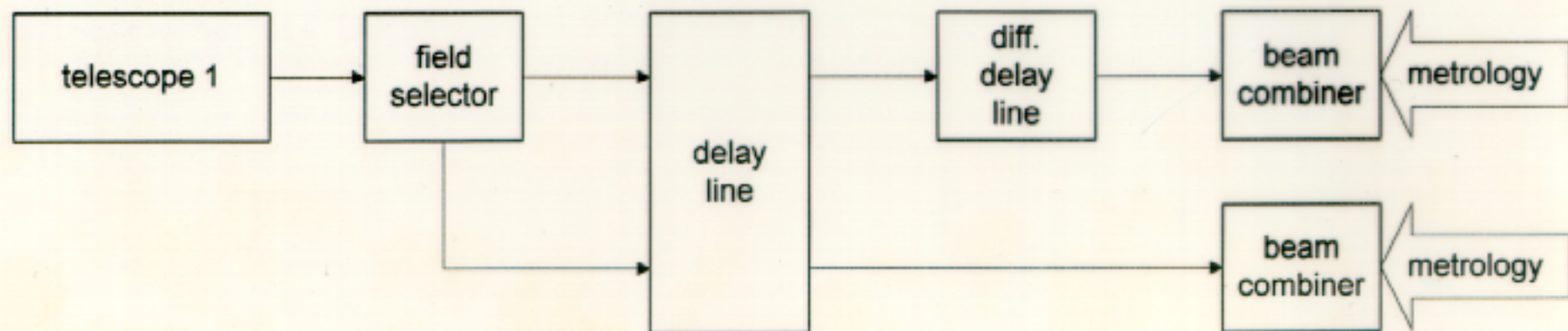
KECK
INTERFEROMETER



Layouts for the dual beam instrument



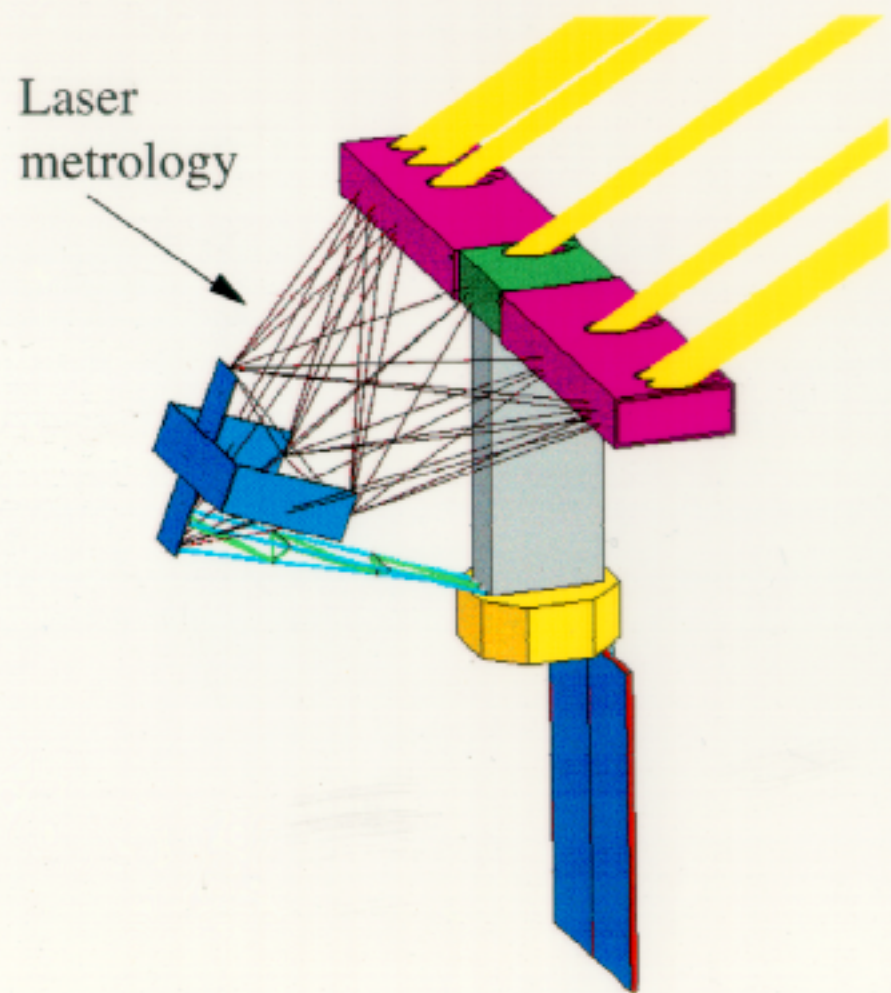
Separated beams



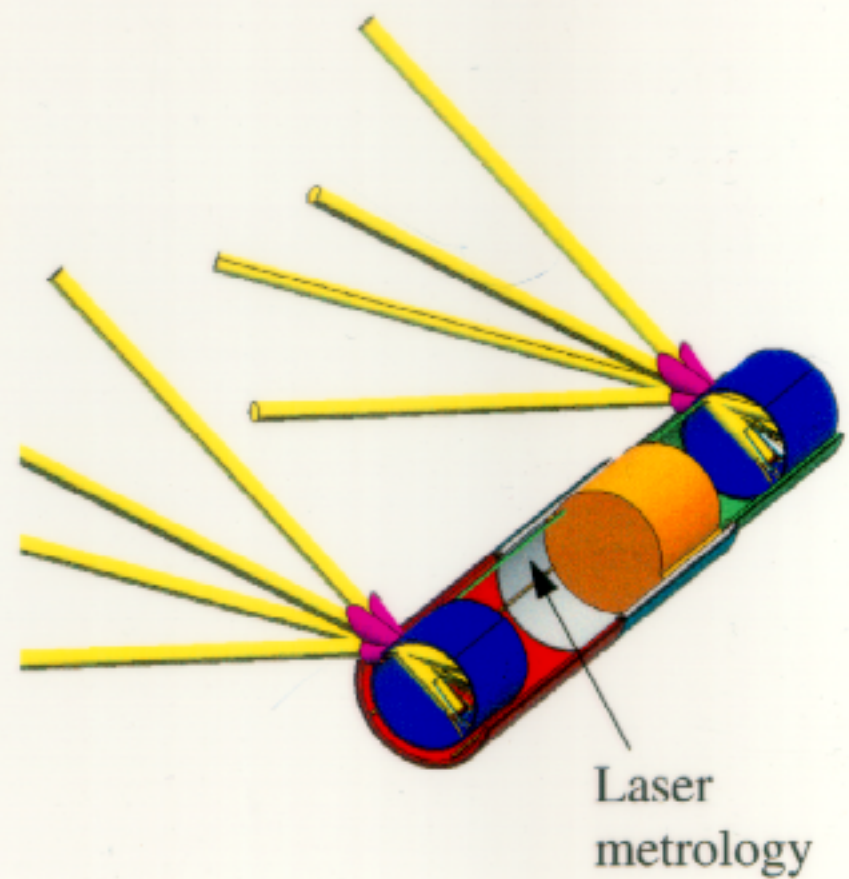
Key Science Topics for Phase-Referenced Imaging

- Active galactic nuclei, radio galaxies and quasars
 - High-redshift galaxies
 - Stellar population in the Galactic Center cluster
 - In general: faint science close to guide stars
 - In addition: observing and fringe tracking at different wavelengths
-

SIM Classic

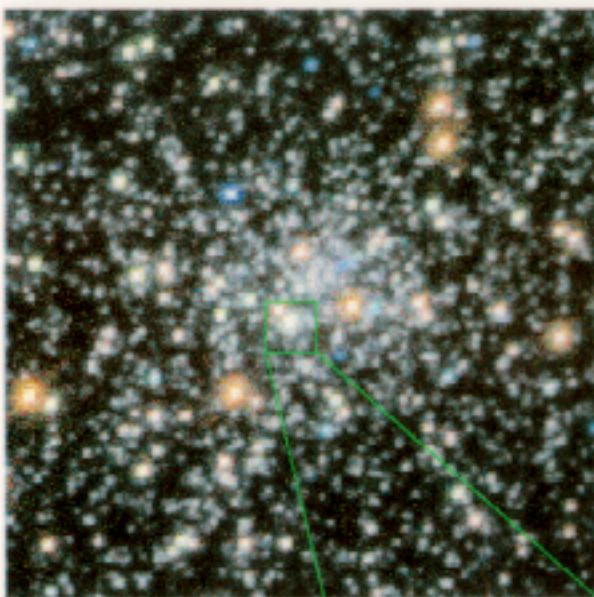


SOS



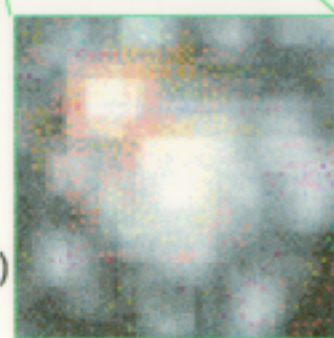
High Resolution Imaging

HST-WFPC2



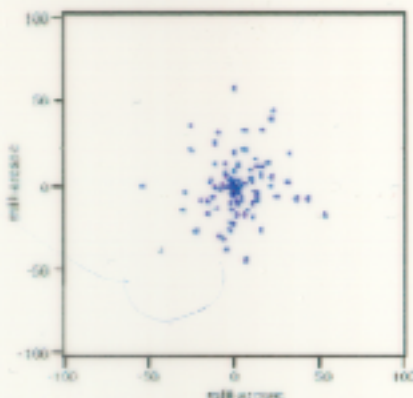
actual field of view
larger than shown

Resolution (FWHM)
53 milliarcsec



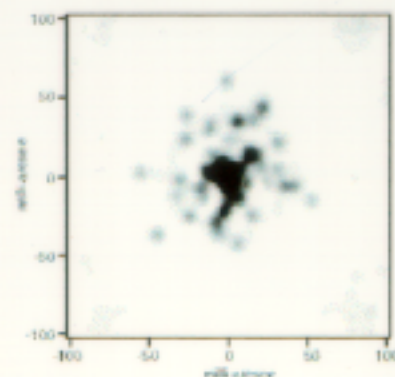
Over small fields of view SIM will show details that currently elude large telescopes. A simulated globular cluster core is used to illustrate this.

Cluster Core Model



"true star positions"

SIM



Resolution (FWHM)
10 milliarcsec

Field of View
0.3 arcsec